



# CHORUS

This is the accepted manuscript made available via CHORUS. The article has been published as:

## Quantum oscillations and criticality in a fermionic and bosonic dimer model for the cuprates

Garry Goldstein, Claudio Chamon, and Claudio Castelnovo

Phys. Rev. B **98**, 184512 — Published 21 November 2018

DOI: [10.1103/PhysRevB.98.184512](https://doi.org/10.1103/PhysRevB.98.184512)

# Quantum oscillations and criticality in a fermionic and bosonic dimer model for the cuprates

Garry Goldstein,<sup>1</sup> Claudio Chamon,<sup>2</sup> and Claudio Castellano<sup>1</sup>

<sup>1</sup>*TCM Group, Cavendish Laboratory, University of Cambridge,  
J. J. Thomson Avenue, Cambridge CB3 0HE, United Kingdom*

<sup>2</sup>*Department of Physics, Boston University, Boston, Massachusetts 02215, USA*

We study quantum oscillations for a system of fermionic and bosonic dimers and compare the results to those experimentally observed in the cuprate superconductors in their underdoped regime. We argue that the charge carriers obey the Onsager quantization condition and quantum oscillations take on a Lifshitz-Kosevich form. We obtain the effective mass and find good qualitative agreement with experiments if we tune the model to the point where the observed mass divergence at optimum doping is associated to a van Hove singularity at which four free-dimer Fermi pockets touch pairwise in the interior of the Brillouin zone. The same van Hove singularity leads to a maximum in the d-wave superconducting pairing amplitude when anti-ferromagnetic interactions are included. Our combined results therefore suggest that a quantum critical point separating the underdoped and overdoped regimes is marked by the location of the van Hove saddle point in the fermionic dimer dispersion.

## I. INTRODUCTION

Recent experiments suggest that the pseudogap phase of the high temperature cuprate superconductors can be described in terms of a vanilla Fermi liquid with an anomalously low quasiparticle density<sup>1-4</sup>. In particular, the observation of quantum oscillations in underdoped cuprates<sup>4-11</sup> with frequency between 500 and 600 T indicates the existence of a Fermi surface with area  $\sim p/8$  (where  $p$  is the doping). What is most convincing evidence of nearly free quasiparticles obeying Fermi-Dirac statistics is the striking resemblance between the amplitude of the oscillations as a function of temperature and that predicted by the Lifshitz-Kosevich formula<sup>4</sup>  $A(T)/A(0) = \pi\eta/\sinh(\pi\eta)$ , where  $\eta = 2\pi k_B T m^*/\hbar e B$  and the effective mass  $m^*$  is the only parameter used to fit experiments over a wide range of temperatures. It is therefore imperative that any candidate model for the cuprates be capable of explaining these features.

A model of fermionic and bosonic (FB) quantum dimers has recently been proposed as a candidate for describing the physics of the underdoped cuprates<sup>12-17</sup>. The FB dimer model contains spinless bosonic dimers, representing a valence bond between two neighboring spins, and spin-1/2 fermionic dimers, representing a hole delocalized between two sites. By condensing the bosonic dimers, one obtains a tractable mean field effective Hamiltonian for the fermionic dimers that captures well the emergence of d-wave superconductivity when the Fermi surface of the dimers exhibits appropriate pockets<sup>15</sup>.

In this paper we study quantum oscillations in the FB quantum dimer model, and compare our results with the behavior experimentally observed in the cuprate superconductors in the underdoped regime. We remark that, although we concentrate on the FB dimer model, the results here presented should apply more generally to systems with degrees of freedom sitting on the bonds, for

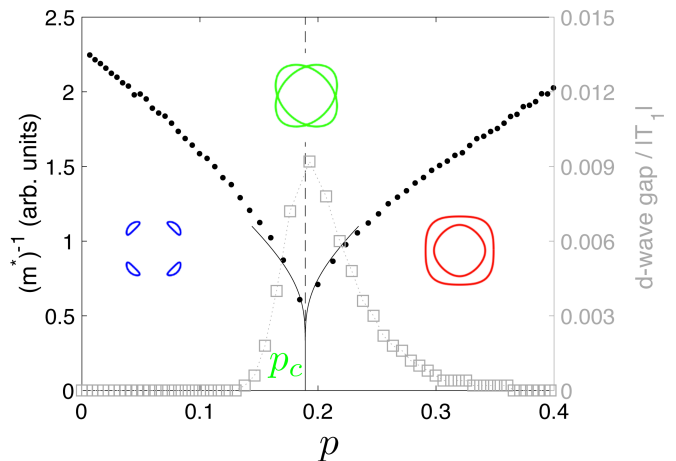


Figure 1. (color online) Inverse quasiparticle mass (circles, left axis) and d-wave superconducting gap (squares, right axis) as a function of the doping  $p$  near the van Hove singularity at  $p_c$  (vertical dashed line), for  $T_2/T_1 = -0.8$ ,  $T_3/T_1 = 0.5$  and  $J/T_1 = 1.0$ . The thin line is the perturbative analytical solution for the inverse mass near the van Hove singularity, as discussed in the text. The data synthesizes our theoretical proposal of a quantum critical point near optimum doping, separating two regimes where the Fermi surface for the fermionic dimers changes between the two topologies shown in blue and red. The critical point is marked by the van Hove singularity, with Fermi surface topology depicted in green.

instance multiorbital models of the cuprates that include the oxygen sites<sup>18</sup>.

In a regime where the magnetic length and the size of the quasiclassical wavepacket is much larger than the lattice spacing, we argue that the fermionic dimers behave as free quasiparticles and undergo semiclassical oscillations under the effect of a magnetic field. These oscillations obey the Onsager quantization condition and the standard Lifshitz-Kosevich form, dictated by the minimal coupling of the gauge field to the quasiparticles.

We compute the effective mass of the quasiparticles and find that it is in good agreement with experiments if we posit that the observed divergence of the mass at optimum doping is associated to a van Hove singularity where the dimer pockets merge in the bulk of the Brillouin zone. Consistently, we find that the superconducting gap and critical temperature are maximal at the value of doping where the Fermi surface topology changes, due to the enhanced density of states at the singularity.

Fig. 1 presents results for the effective mass and superconducting order parameter as function of doping. This data summarizes our proposal of a quantum critical point near optimum doping, separating two regimes where the Fermi surfaces for the fermionic dimers have different topology, as depicted in the figure. The quantum critical point corresponds to a van Hove singularity *inside* the Brillouin zone, *not* at its boundary.

Together with earlier work<sup>12-17</sup>, our results make a substantial contribution to highlight the suggestive similarity between the behavior of the FB dimer model and the physics of underdoped cuprates near the superconducting dome. This is most remarkable given the relative simplicity of the effective dimer description. Whereas the FB dimer model comes with a number of free parameters that are difficult to fix from first principles, our work imposes strong limitations on the range of these parameters where the behavior of the model compares well with experiments. This brings us within reach of critically testing the validity and limits of this model to describe the behavior of underdoped cuprates.

## II. THE EFFECTIVE MODEL

In our study of quantum oscillations, we consider the mean field description presented in Ref. 15 of the FB dimer model introduced in Ref. 12 to describe the pseudogap phase of the underdoped cuprates. Substantial progress in understanding the fermionic component of the theory can be made using the mean field Hamiltonian obtained by condensing bosonic dimer bilinears, which renormalize the effective hopping amplitudes for the remaining fermionic dimers (illustrated pictorially in Fig. 2). The approach is phenomenological, in that we do not compute these amplitudes microscopically, but instead we treat them as free fitting parameters  $T_{1,2,3}$ .

The fermionic mean field Hamiltonian reads<sup>15</sup>:

$$\begin{aligned}
H_{F\bar{B}} = & -T_1 \sum_i \sum_{\sigma} \left( c_{i+\hat{y},\hat{x},\sigma}^{\dagger} c_{i,\hat{x},\sigma} + c_{i+\hat{x},\hat{y},\sigma}^{\dagger} c_{i,\hat{y},\sigma} \right) + \text{H.c.} \\
& -T_2 \sum_i \sum_{\sigma} \sum_{v \in V_2} c_{i+v,\hat{y},\sigma}^{\dagger} c_{i,\hat{x},\sigma} + \text{H.c.} \\
& -T_3 \sum_i \sum_{\sigma} \sum_{v \in V_3} c_{i+v,\hat{y},\sigma}^{\dagger} c_{i,\hat{x},\sigma} + \text{H.c.} \\
& -\mu \sum_i \sum_{\sigma} \left( c_{i,\hat{x},\sigma}^{\dagger} c_{i,\hat{x},\sigma} + c_{i,\hat{y},\sigma}^{\dagger} c_{i,\hat{y},\sigma} \right). \quad (1)
\end{aligned}$$

The operator  $c_{i,\eta,\sigma}$  annihilates a fermion with spin  $\sigma$  on

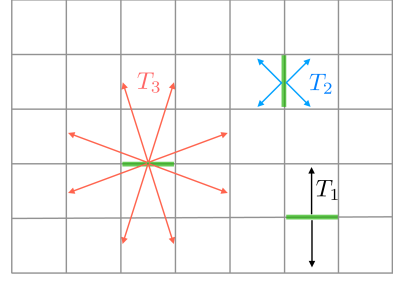


Figure 2. (color online) The FB quantum dimer model of Ref. 12 contains dimers on the bonds of the square lattice. Condensing the bosonic dimers leads to a theory of free fermionic dimers, Eq. (1), with effective hoppings  $T_{1,2,3}$  that encode both the bare coupling constants and the expectation values of bilinears in the bosonic dimers, as presented in Ref. 15. The lattice of bonds contains two sublattices, corresponding to the vertical and horizontal bonds. The hopping amplitudes  $T_{2,3}$  moves dimers between the two sublattices, while hopping amplitude  $T_1$  breaks chiral symmetry.

the bond  $(i, i + \eta)$ , which is horizontal for  $\eta = \hat{x}$  or vertical for  $\eta = \hat{y}$ . Notice that  $T_1$  hops the fermionic dimers between parallel bonds, while  $T_{2,3}$  flip the dimers from horizontal to vertical and *vice versa*. We define (in momentum space) the spinor that encodes the horizontal and vertical flavors as  $\psi_{\vec{k},\sigma}^{\dagger} = (c_{\vec{k},\hat{y},\sigma}^{\dagger}, c_{\vec{k},\hat{x},\sigma}^{\dagger})$  and<sup>15</sup>:

$$H_{F\bar{B}} = \sum_{\vec{k},\sigma} \psi_{\vec{k},\sigma}^{\dagger} \begin{pmatrix} \xi_{\vec{k}}^x & \gamma_{\vec{k}} \\ \gamma_{\vec{k}}^* & \xi_{\vec{k}}^y \end{pmatrix} \psi_{\vec{k},\sigma}, \quad (2)$$

where:

$$\begin{aligned}
\xi_{\vec{k}}^{x,y} &= -\mu - 2T_1 \cos k_{x,y} \\
\gamma_{\vec{k}} &= 4 e^{i(k_y - k_x)/2} \left( T_2 \cos \frac{k_x}{2} \cos \frac{k_y}{2} \right. \\
& \quad \left. + T_3 \cos \frac{3k_x}{2} \cos \frac{k_y}{2} + T_3 \cos \frac{k_x}{2} \cos \frac{3k_y}{2} \right).
\end{aligned}$$

The eigenvalues are given by  $E_{\pm, \vec{k}} = \xi_{\vec{k}} \pm \sqrt{\eta_{\vec{k}}^2 + |\gamma_{\vec{k}}|^2}$ , where  $\xi_{\vec{k}} = (\xi_{\vec{k}}^x + \xi_{\vec{k}}^y)/2$  and  $\eta_{\vec{k}} = (\xi_{\vec{k}}^x - \xi_{\vec{k}}^y)/2$ . The lower band  $E_{-, \vec{k}}$  will be partially occupied upon hole doping, with concentration  $p$ .

We shall rescale the Hamiltonian and study  $H_{F\bar{B}}/|T_1|$ , i.e., work in energy units of  $|T_1| = 1$ . We proceed with our investigation of the model by analyzing its properties as a function of the dimensionless ratios  $T_2/|T_1|$  and  $T_3/|T_1|$ , as well as the doping  $p$  (controlled by the chemical potential  $\mu$ ). The essence of our approach is to determine the space of parameters of the system where it matches the phenomenology of the cuprates. For instance, in Ref. 15 it was found that the region in the two dimensional parameter space exhibiting four small Fermi pockets largely overlapped with the region where d-wave superconductivity existed, when the anti-ferromagnetic coupling  $J$  of the  $t - J$  model was included. We note

that the state with the lower band fully occupied corresponds to an unphysical doping  $p = 2$ ; however, the physics discussed in this paper pertains to sensibly small values of the hole doping  $p$  where one can expect the dimer representation to be valid.

### III. QUANTUM OSCILLATIONS

Oscillations of magnetoresistance reflect how a system responds to an applied magnetic field, which always couples minimally to the physical constituents of the system, i.e., electrons. The fermionic dimers are not the elementary constituents; they are emerging particles, and therefore the case for quantum oscillations requires more care.

The Hamiltonian Eq. (1) is obtained from a mean field approximation of an interacting FB dimer model, which in turn is an effective projection of a microscopic system, such as the Hubbard model, onto a subspace of dimers. Thus we are faced with the problem of logically justifying that the mean field Hamiltonian does capture quantum oscillations of the underlying physical system.

The justification for minimally coupling the dimers to the external magnetic field hinges on the fact that we restrict our analysis to the case when the dimer size (set by the lattice spacing) is much smaller than both the magnetic length and the size of the wavepacket. In other words, in this regime one cannot resolve the non-elementary nature of the fermionic dimers. Hence, quantum oscillations in the FB dimer model are described by those of charged quasiparticles with dynamics governed by Eq. (1) upon shifting  $\vec{k}$  by the gauge potential. In this regime, it is therefore reasonable to expect the quantum oscillations to satisfy the Onsager quantization condition as well as the Lifshitz-Kosevich formula.

We note that the conventional expectation for the charge of fermionic dimers in the FB model is  $+e^{12}$ . This sign is consistent with Hall coefficient measurements at high temperature. However, the data show a change of sign of the carriers at low temperatures<sup>3,19</sup>. Understanding this phenomenon is beyond the scope of the present paper, but an explanation may be possible within the FB dimer model if one accounts for phase factors in the wave function of the bosonic dimers in presence of sufficiently large magnetic fields.

One of the salient features of the mean field model governed by Eq. (1) is a region in parameter space  $T_{1,2,3}$  where the dispersion exhibits pockets near the  $(\pm\pi/2, \pm\pi/2)$  points. The period of oscillations depends on the size of the Fermi surfaces, with each disconnected surface contributing its own frequency. The presence of 4 identical Fermi pockets of size  $p/8$  (the factor of 2 due to spin) is consistent with the experimental data<sup>4,9,10</sup> in the doping range of 10-16%, with the  $p/8$  result being a nearly ideal intercept at a doping of  $\sim 13\%$ . The slope of the  $p/8$  curve is higher than the slope of the experimental data with the frequency of oscillations between 500-600 Tesla in the doping range of 10-16%; however the

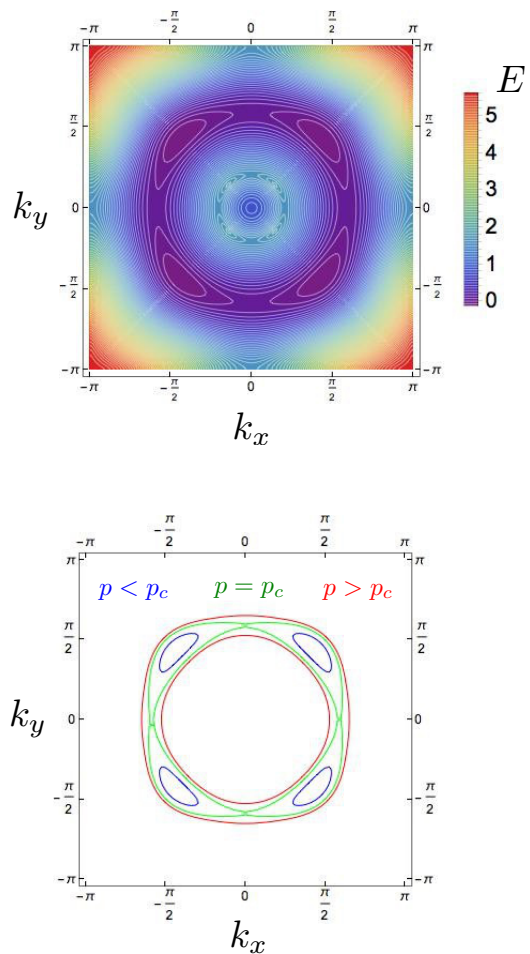


Figure 3. (color online) Dispersion for the effective model of fermionic dimers for  $T_2/T_1 = -0.8$  and  $T_3/T_1 = 0.5$ . Top panel: constant energy surfaces, with  $E = 0$  measured from the bottom of the band near  $(\pm\pi/2, \pm\pi/2)$ . Bottom panel: Fermi surfaces corresponding to doping levels slightly below, at, and slightly above optimum doping  $p_c$ , where saddle points in the energy dispersion occur near  $(0, \pm\pi/2)$  and  $(\pm\pi/2, 0)$ .

discrepancy is small (see Appendix B).

Experimentally, the oscillations become less well defined as one approaches optimal doping. In addition, experimental measurements show that the effective quasiparticle mass increases as the density increases towards the optimal doping value, with the extrapolation suggesting a divergence. This is consistent with the presence of a Fermi surface singularity, where quantum oscillations are suppressed because of the corresponding enhancement in the density of states and the residual interactions, not captured by mean field theory, lead to scattering and departure from the Lifshitz-Kosevich formula.

Here we explore the possibility that this suppression of quantum oscillations near optimal doping corresponds to a new type of van Hove singularity for the cuprates where the four pockets merge in the bulk of the Brillouin zone, morphing into two Fermi surfaces with one sheathing the other (as illustrated in the bottom panel of Fig. 3).

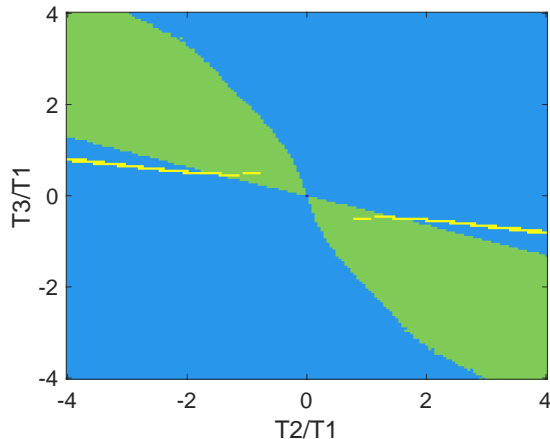


Figure 4. (color online) s-wave (blue) vs d-wave (green) phase diagram of the mean field fermionic dimer model in presence of antiferromagnetic interaction  $J/T_1 = 50$ , where we have chosen  $T_1 > 0$ . Highlighted in yellow is the locus of the points in the  $T_2/T_1$ ,  $T_3/T_1$  plane where the van Hove singularity occurs for  $p \in (0.18, 0.22)$ . Notice the small but finite overlap with the d-wave region, near  $T_2/T_1 \simeq \mp 0.8$  and  $T_3/T_1 \simeq \pm 0.5$ .

Notice that this singularity is different in nature with respect to the ones previously studied in the context of underdoped cuprates<sup>18</sup> in two main aspects: it does not arise from the competition with an ordering instability (e.g., CDW), and it takes place away from the Brillouin zone boundary.

For our proposed scenario to occur, we ought to find a region in parameter space of the mean field model where: (i) the dispersion exhibits four pockets; (ii) the targeted van Hove singularity occurs near  $p = 0.2$  (say within  $\pm 0.02$ ); and (iii) the leading superconducting instability in presence of interactions is d-wave.

We find that the model is able to satisfy the conditions (i) and (ii) in a small sliver in the  $T_2/T_1$ ,  $T_3/T_1$  plane (see Fig. 4), only if we choose the sign of  $T_1$  to be positive.

In order to assess whether any portion of the identified sliver is consistent with the model exhibiting d-wave superconductivity, we consider the effect of the antiferromagnetic interaction  $J$  of the  $t-J$  model from which the FB model descends, and follow the procedure in Ref. 15 to compare s-wave vs d-wave free energies. The choice of value of the ratio  $J/T_1$  of interaction strength  $J$  to the scale  $T_1$  is non trivial, since in our phenomenological approach we do not determine  $T_1$  from first principles. (The value of  $T_1$  can be much smaller than the value of  $t$  because of the suppression coming from the condensation of the bosonic dimers.) However, we find – as it is reasonable to expect – that the phase boundaries between s-wave and d-wave as a function of system parameters become independent of  $J$  when  $J/T_1 \gg 1$ , and the latter in general favors d-wave superconductivity. For this reason we opted to work in the large  $J/T_1$  limit and thus obtain an upper bound to the portion of parameter space

where (i), (ii) and (iii) are satisfied. This is illustrated in Fig. 4 by the overlap between the sliver and the d-wave portion of the phase diagram (shown for  $J = 50$  in units of  $T_1$ ). What we find is a narrow but non-vanishing region in parameter space, located around  $T_2/T_1 = \mp 0.8$ ,  $T_3/T_1 = \pm 0.5$ . The dispersion of the system at these points is shown in the top panel in Fig. 3.

When a van Hove singularity occurs in a 2D fermionic systems, the effective mass of the quasiparticle excitations diverges logarithmically as

$$m^* \sim a \log \frac{\Lambda}{|\varepsilon|}, \quad (3)$$

where  $\varepsilon$  is the energy from the Van-Hove singularity,  $\Lambda$  is the bandwidth, and  $a$  has dimensions of mass. The inverse mass as a function of  $p$  is also shown for  $T_2/T_1 = -0.8$  and  $T_3/T_1 = 0.5$  in Fig. 1. Near the van Hove singularity, it is possible to obtain a perturbative analytical expression that relates the inverse mass to the doping,

$$|p - p_c| = b \left( \frac{m^*}{a} + 1 \right) e^{-m^*/a}, \quad (4)$$

where  $a \simeq 0.25$  and  $b \simeq 0.38$  are found most conveniently by fitting to the numerical data (thin line near  $p_c$  in Fig. 1).

We further checked that d-wave is the leading superconducting instability for these values of  $T_2/T_1$ ,  $T_3/T_1$ , for a range of values of  $J/T_1$  (see the Supplementary Online Information). We find that the superconducting gap  $\Delta$  scales as  $\Delta \sim 0.02J$ . In Fig. 1 we show the value of the superconducting gap for  $J = 1.0$  in units of  $T_1$ . This choice takes into account that the ratio  $J/t \sim 0.2 - 0.4$ , and that  $T_1/t$  is similarly suppressed with respect to  $t$ .

As discussed above, and illustrated in Fig. 3, the van Hove singularity considered here separates a region with 4 identical Fermi pockets of size  $p/8$  from a region with two (much larger) Fermi surfaces, with one surface enclosing the other. We therefore expect two distinct features as the system crosses the singularity: (a) a discontinuous jump in the period of oscillations; and (b) the appearance of two (much smaller) distinct periods for  $p > p_c$ . However, it may well happen that the experimental validity of the FB dimer model does not extend to the overdoped regime and breaks down at  $p_c$ . Further work beyond the scope of the present paper is needed to ascertain this possibility and investigate alternative scenarios as  $p$  is tuned across the singularity.

#### IV. CONCLUSIONS

In this work we studied quantum oscillations in a FB dimer model for high temperature superconductors, within a mean field approximation. We argued that our system satisfies Onsager quantization and the Lifshitz-Kosevich formula. We studied the effective mass for

quantum oscillations and found that it diverges at a van Hove singularity where four Fermi pockets merge pairwise at a critical doping at four different points in the Brillouin zone. The location of the singularity depends on the effective fermionic dimer hopping parameters, and we narrowed down the range of such parameters for the model to contain pockets in the underdoped regime, display d-wave superconductivity, and have the singularity near optimal doping  $p \sim 0.2$ .

We find that we can match rather well the experimental quantum oscillation behavior in the cuprates. This is remarkable given the simplicity of the effective dimer model. It is furthermore enticing that the agreement occurs for a relatively narrow range in parameter space; our results bring us closer to propose a comparison of the behavior of the mean field dimer model with experiments that will critically ascertain its limits of validity.

One of the predictions we make is that across the van Hove singularity the quantum oscillation frequency jumps discontinuously to much larger values and two periods appear. The current state-of-the-art high-field capability does not allow one to study quantum oscillations near optimum doping in the cuprates to verify this prediction. However, it may well be within range of near future improvements in the experimental technique.

The enhanced density of states at the van Hove singularity consistently coincides with a maximum in the superconducting gap at the value of doping corresponding to that where the Fermi surface topology changes. This result supports a theoretical proposal of a quantum critical point near optimum doping associated with a van Hove singularity where four Fermi pockets merge inside the Brillouin zone (not at its boundary). Fig. 1 highlights our proposed scenario. We expect this finding to have observable consequences in the quantum critical region, for instance on the temperature dependence of the resistivity. Our results thus give a concrete motivation to study quantum criticality at a van Hove singularity.

*Acknowledgements.* We are very grateful to Nigel Cooper for many useful discussions that helped us shape this project and understand the nature of quantum oscillations in the fermion boson dimer model. This work was supported, in part, by the Engineering and Physical Sciences Research Council (EPSRC) Grant No. EP/M007065/1 (C.Ca. and G.G.), and by DOE Grant No. DE-FG02-06ER46316 (C.Ch.). Statement of compliance with the EPSRC policy framework on research data: this publication reports theoretical work that does not require supporting research data.

## Appendix A: Superconducting gap and inverse mass

In Fig. 5 we verify that the d-wave superconducting instability is the leading instability for  $T_2/T_1 = -0.8$  and  $T_3/T_1 = 0.5$ , for a range of values of the interaction  $J$ .

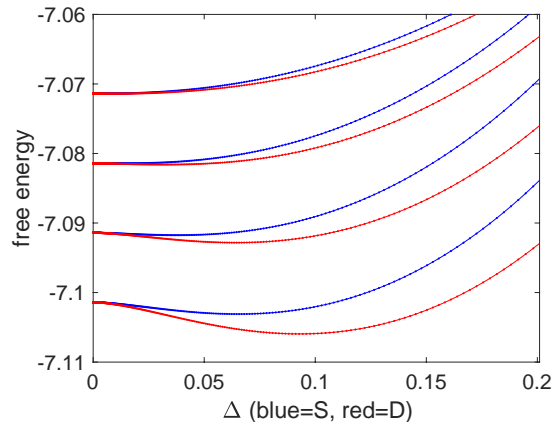


Figure 5. (color online) Comparison of s-wave (blue) vs d-wave (red) free energies as a function of the gap  $\Delta$  for  $T_2/T_1 = -0.8$  and  $T_3/T_1 = 0.5$ , for  $J/T_1 = 1.5, 2.5, 3.5, 4.5$  (top to bottom pairs of curves). The value of the chemical potential was chosen near the van Hove saddle point. An artificial offset has been introduced (with respect to the bottom pair of curves) for visualization purposes. Without offset, all the curves coincide at  $\Delta = 0$ . In all cases (although it is difficult to see for small values of  $J$  in the figure), the minimum of the d-wave free energy occurs at a finite value of  $\Delta$  and is lower than the minimum of the s-wave free energy.

The mean field dimer model ceases to be a good representation of the original FB dimer model, and even more so of the underlying electronic system, when the density of fermionic dimers  $p$  increases. With this caveat in mind, we show for completeness in Fig. 6 the behavior of the inverse mass of the mean field dimer model over a larger interval in  $p$ . Further van Hove singularities occur for  $p > 0.8$  (not shown). In Fig. 7 we then show the behavior of the d-wave gap on the broader range of  $p$ , for different values of  $J$ . We note that larger values of  $J$  tend to mix the small  $p$  behavior with the large  $p$  behavior of the model (namely, other van Hove singularities for  $p > 0.8$ ) and therefore they ought to be considered with care.

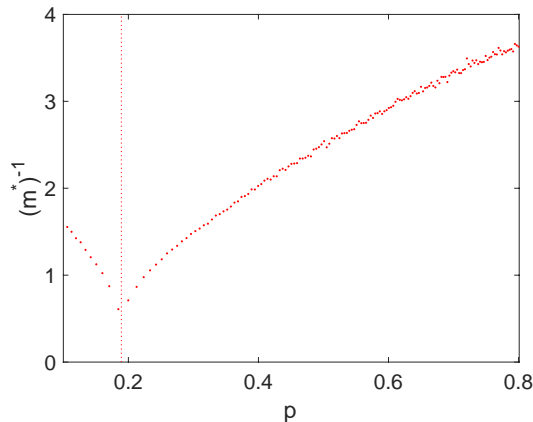


Figure 6. Inverse quasiparticle mass for  $p \in (0, 0.8)$  at  $T_2/T_1 = -0.8$  and  $T_3/T_1 = 0.5$ . The vertical dotted line indicates the position of the van Hove singularity considered in the main text. (These are the same data shown in Fig. 1 of the main text for a narrower range of doping.)

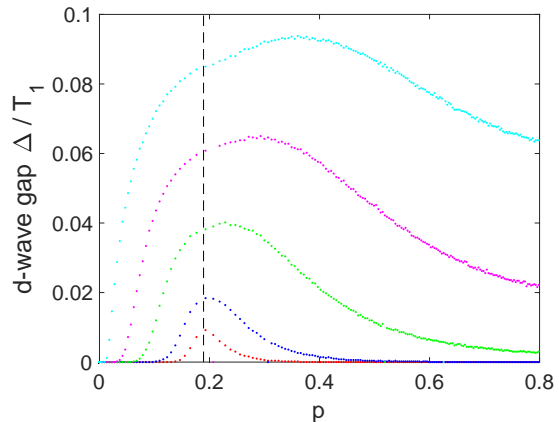


Figure 7. (color online) d-wave gap  $\Delta/T_1$  for  $T_2/T_1 = -0.8$ ,  $T_3/T_1 = 0.5$  and  $J/T_1 = 1.0, 1.5, 2.5, 3.5, 4.5$  (red, blue, green, magenta, cyan). The vertical dashed line indicates the location of the van Hove singularity.

From Fig. 7 we observe that the dependence of the maximum value of  $\Delta(p)/T_1$  on the coupling strength  $J/T_1$  is approximately linear, following the relation  $\Delta \sim 0.02J - 0.01$  reported in the main text.

## Appendix B: Frequency of the oscillations

If we assume a Fermi surface of area  $p/8$  and a lattice constant of  $3.8 \text{ \AA}$ , we find that the frequency of oscillations  $F$  (measured in Tesla) is related to the doping  $p$  in the cuprates as:

$$F = 3.58 \cdot 10^3 \cdot p. \quad (\text{B1})$$

According to this relation, a typical frequency of 530 Tesla corresponds to  $p = 0.148$ . Eq. (B1) is com-

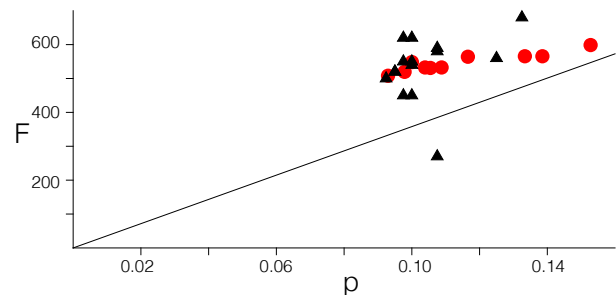


Figure 8. Frequency  $F$  of the quantum oscillations (in Tesla) as a function of doping  $p$  from two independent experimental groups (Ref. 9 in red and Ref. 10 in black). The black solid line is Eq. (B1).

pared to experimental quantum oscillations data from Ramshaw et al.<sup>10</sup> (red dots) and from Singleton (black triangles) et al.<sup>9</sup> in Fig. 8.

- 
- <sup>1</sup> S. I. Mirzaei, D. Stricker, J. N. Hancock, C. Berthod, A. Georges, E. van Heumen, M. K. Chan, X. Zhao, Y. Li, M. Greven, N. Barišić, and D. van der Marel, Proc. Nat. Acad. Sci. **110**, 5774 (2013).
- <sup>2</sup> M. K. Chan, M. J. Veit, C. J. Dorow, Y. Ge, Y. Li, W. Tabis, Y. Tang, X. Zhao, N. Barišić, and M. Greven, Phys. Rev. Lett. **113**, 177005 (2014).
- <sup>3</sup> D. LeBoeuf, N. Doiron-Leyraud, J. Levallois, R. Daou, J.-B. Bonnemaïson, N. E. Hussey, L. Balicas, B. J. Ramshaw, R. Liang, D. A. Bonn, W. N. Hardy, S. Adachi, C. Proust and L. Taillefer, Nature **450**, 533 (2007).
- <sup>4</sup> S. E. Sebastian, N. Harrison and G. G. Lonzarich, Phyl. Trans. of Royal Soc. A **369**, 1687 (2011).
- <sup>5</sup> N. Doiron-Leyraud, C. Proust, D. LeBoeuf, J. Levallois, J.-B Bonnemaïson, R. Liang, D. A. Bonn, W. N. Hardy and L. Taillefer, Nature **447**, 565 (May 2007).
- <sup>6</sup> A. F. Bangura, J. D. Fletcher, A. Carrington, J. Levallois, M. Nardone, B. Vignolle, P. J. Heard, N. Doiron-Leyraud, D. LeBoeuf, L. Taillefer, S. Adachi, C. Proust, and N. E. Hussey, Phys. Rev. Lett. **100**, 047004 (2008)
- <sup>7</sup> C. Jaudet, D. Vignolles, A. Audouard, J. Levallois, D. LeBoeuf, N. Doiron-Leyraud, B. Vignolle, M. Nardone, A. Zitouni, R. Liang, D. A. Bonn, W. N. Hardy, L. Taillefer, and C. Proust Phys. Rev. Lett. **100**, 187005 (2008).
- <sup>8</sup> S. E. Sebastian, N. Harrison, M. M. Altrawneh, C. H. Mielke, R. Liang, D. A. Bonn, W. N. Hardy and G. G. Lonzarch, Proc. Nat. Acad. Sci. **107**, 6175 (2010).
- <sup>9</sup> J. Singleton, C. de la Cruz, R. D. McDonald, S. Li, M. Altrawneh, P. Goddard, I. Franke, D. Rickel, C. H. Mielke, X. Yao, and P. Dai, Phys. Rev. Lett. **104**, 086403 (2010)
- <sup>10</sup> B. J. Ramshaw, S. E. Sebastian, R. D. McDonald, J. Day, B. S. Tan, Z. Zhu, J. B. Betts, R. Liang, D. A. Bonn, W. N. Hardy, N. Harrison, Science **348**, 317 (2015).
- <sup>11</sup> N. Barišić, S. Badoux, M. K. Chan, C. Dorow, W. Tabis, B. Vignolle, G. Yu, J. Béard, X. Zhao, C. Proust and M. Greven, Nature Physics **9**, 761 (2013).
- <sup>12</sup> M. Punk, A. Allais and S. Sachdev, Proc. Nat. Acad. Sci. **112**, 9552 (2015).
- <sup>13</sup> D. Chowdhury and S. Sachdev *The enigma of the pseudogap phase in the cuprate superconductors in Quantum criticality in condensed matter: phenomena, materials and ideas in theory and experiment* J. Jędrzejewski eds. (World Scientific Publishing co, Singapore 2016).
- <sup>14</sup> A. A. Patel, D. Chowdhury, A. Allais, and S. Sachdev, Phys. Rev. B **93**, 165139 (2016).
- <sup>15</sup> G. Goldstein, C. Chamon and C. Castelnovo, Phys. Rev. B **95**, 174511 (2017).
- <sup>16</sup> J. Feldmeier, S. Huber, M. Punk, arXiv 1712.01854.
- <sup>17</sup> S. Huber, J. Feldmeier, M. Punk, arXiv 1710.00012.
- <sup>18</sup> V. J. Emery, Phys. Rev. Lett. **58**, 2794 (1987).
- <sup>19</sup> D. LeBoeuf, N. Doiron-Leyraud, B. Vignolle, M. Sutherland, B. J. Ramshaw, J. Levallois, R. Daou, F. Laliberté, O. Cyr-Choinière, J. Chang, Y. J. Jo, L. Balicas, R. Liang, D. A. Bonn, W. N. Hardy, C. Proust, and L. Taillefer, Phys. Rev. B **83**, 054506 (2011).